Front. Optoelectron. 2017, 10(3): 299–307
DOI 10.1007/s12200-017-0719-3

RESEARCH ARTICLE

Microperforation of the human nail plate by radiation of erbium lasers

Andrey V. BELIKOV (✉), Andrey N. SERGEEV, Sergey N. SMIRNOV, Anastasia D. TAVALINSKAYA

Department of Laser Technologies and Systems, Saint-Petersburg National Research University of Information Technologies, Mechanics and Optics (ITMO University), Saint Petersburg 197101, Russia

Abstract The nail plate forms a barrier that limits the effectiveness of drug delivery in the treatment of nail diseases and prevents the outflow of fluid in the case of subungual hematoma formation. Microperforation of the nail plate through laser radiation can increase the effectiveness of drug delivery and ensure the possibility of blood outflow.

This study detected and identified the type and threshold of effects that arise from exposing the nail plate to Yb,Er:Glass (λ = 1.54 μm) and Er:YLF (λ = 2.81 μm) laser radiation. The rate and efficiency of nail plate ablation by the radiation of these lasers were studied. The effect of the storage time of a freshly extracted nail plate in open air on its ablation rate by Er:YLF (λ = 2.81 μm) laser radiation was also investigated.

The impact of the Yb,Er:Glass and Er:YLF laser pulses on the nail plate caused bleaching, carbonization, ablation with microcrater formation, and microperforation. The laser energy densities W_E (thresholds) required for these effects were determined. The maximum ablation rate for Yb,Er:Glass laser radiation was 8 μm/pulse at $W_E = 91 \pm 2$ J/cm^2, whereas that for Er:YLF laser radiation was 12 μm/pulse at $W_E = 10.5 \pm 0.5$ J/cm^2. The maximum ablation efficiency for Yb,Er:Glass laser radiation was 0.1 μm/mJ at $W_E = 10.5 \pm 0.5$ J/cm^2, whereas that for Er:YLF laser radiation was 4.6 μm/mJ at $W_E = 5.3 \pm 0.3$ J/cm^2. The laser ablation rate depends on the storage time and conditions of the freshly extracted nail plate. For example, when exposed to Er:YLF laser radiation, the laser ablation rate decreased by half from the initial maximum value in 96 h of air storage and returned to the initial value after 1 h of storage in distilled water.

Keywords Yb, Er:Glass laser, Er:YLF laser, nail plate, microperforation, ablation rate, ablation efficiency, dehydration

Received March 31, 2017; accepted May 10, 2017

E-mail: meddv@grv.ifmo.ru

1 Introduction

Nail surgery is a common procedure in dermatology. The most common reasons why a patient consults a dermatologist are subungual hematoma, onychomycosis (fungal infection), and nail psoriasis. These diseases are widespread among the population, especially among the elderly and people with compromised immunity.

A local treatment is the most favorable option for patients because of its non-invasiveness and elimination of systemic therapy-associated side effects, such as allergic reactions, rashes, and gastrointestinal upsets. However, local therapy is ineffective due to the low permeability of the nail plate for drugs (i.e., less than 0.2% of the applied dose of drugs reaches the nail bed) [1]. Therefore, the effectiveness of photodynamic therapy, ozone therapy, ionophoresis, laser therapy, and other treatment methods also decreases [2,3].

Different methods have been employed to increase the effectiveness of local treatment. Mechanical methods involve the surgical removal or abrasive grinding of the nail plate [2,4]. However, healing after such surgical interference takes a long time, and the probability of reinfection and damage to the nail matrix is high [5]. Chemical methods involve etching the nail plate due to the destruction of the disulfide, peptide, hydrogen, and polar bonds of keratin. For the destruction of sulfites, hydrogen peroxide, urea, salicylic acid, and different keratolic enzymes are employed. For example, an 88% phenol solution can be utilized, followed by phenol neutralization with ethyl, isopropyl alcohol, alcohol solution of povidone–iodine, 10% NaOH solution, and 20% solution of tartaric acid or 10% phosphoric acid [6]. Chemical etching takes considerable time to complete [7], and a

weak chemical effect leads to extensive chemical burns and tissue necrosis.

Microperforation has been actively developing recently. This method consists of the creation of a microhole array in the nail plate [8]. Microholes in the nail plate increase the effectiveness of drug delivery to the nail bed and accelerate the treatment process [2,8,9]. This method is low-traumatic and characterized by minor bleeding as well as short and comfortable recovery period. Microperforation of the nail plate can also be applied to provide blood outflow in the case of subungual hematoma formation [10].

A red-hot metal needle is usually used for microperforation of the nail plate [11,12]. This microperforation method is painful for the patient and is utilized, as a rule, to create single holes [11]. Microcutting devices destroy the nail plate with the help of drills and can be employed to create a microhole array [2]. Holes in the nail plate can also be created by chemical etching [6] or by low-frequency ultrasound [2]. Chemical etching is traumatic, and the ultrasonic method requires fluid delivery to the nail plate [2].

Microholes in the nail plate can be created by laser radiation. Among the advantages of laser microperforation of the nail plate over the aforementioned methods include distinguishing asepticity, ablasticity, low probability of reinfection, minimal damage of surrounding tissues, and the consequent rapid recovery of the patient [6,13]. Microperforation of the nail plate by laser radiation occurs at a high speed [2,8,14–16]. Thus, laser microperforation of the nail plate is a promising direction in the treatment of onychomycosis, nail psoriasis, and subungual hematoma.

In 1997, Neev et al. [14] conducted a comparative study of nail plate ablation through Er:YAG, Ti:Sapphire, XeCl, and Ho:YSGG laser radiation. The highest ablation rate of the nail plate (up to 30 μm/pulse) was observed after exposure to Er:YAG laser radiation, and the highest ablation efficiency of the nail plate was observed after exposure to femtosecond Ti:Sapphire laser radiation (up to 1 μm/mJ). Ablation of the nail plate by Er:YAG laser radiation was also investigated in Ref. [15]. Data on the destruction of the nail plate by CO_2 [2,8,16] laser radiation and onychomycosis therapy with Nd:YAG [17,18] laser are also available.

The present study investigates the possibility of using Yb,Er:Glass (λ = 1.54 μm) and Er:YLF (λ = 2.81 μm) lasers for the microperforation of the human nail plate. Interest in these laser sources is associated with the possibility of realizing effective diode pumping in them. Diode pumping decreases the size of laser systems and facilitates the control of energy and time parameters of laser radiation. Moreover, the wavelengths of these lasers belong to intense absorption bands of water contained in the nail plate. However, no data on the impact of Yb,Er: Glass and Er:YLF laser radiation on the nail plate currently exist.

Hence, our in vitro investigation attempts to study the effects that arise from exposing the nail plate to Yb,Er: Glass (λ = 1.54 μm) and Er:YLF (λ = 2.81 μm) laser radiation, study the rate and efficiency of nail plate ablation by the radiation of these lasers, and investigate the effect of the storage time of a freshly extracted nail plate in open air on the ablation rate by Er:YLF (λ = 2.81 μm) laser radiation.

2 Materials and methods

In vitro samples of human nail plate were used in the experiment. The samples were obtained from five volunteers aged 20–30 years old (2 males and 3 females). A total of 160 samples of nail plates were obtained for the experiment. After extraction, the samples were stored in open air at room temperature for a maximum of 30 days. The average thickness of the samples was 370±15 μm. After cleaning and drying (at least 5 days at room temperature), nail plates were placed in the focal plane of the convex lens. Averaging over 10 samples was carried out for each experimental point to consider the effect of individual nail properties.

The scheme of the experimental setup to process the nail plate with Yb,Er:Glass laser radiation is shown in Fig. 1(a). The cavity of the flash-lamp pumped Yb,Er:Glass laser was formed by three high-reflectivity mirrors. The laser operated in the cavity-dumping mode. Useful losses were modulated by a frustrated total internal reflection (FTIR) shutter in such scheme, which provided the radiation output from the cavity. The Fresnel attenuator was utilized to change the laser pulse energy while saving its duration and temporal structure. The total Yb,Er:Glass laser pulse duration (on the basis) was 4.5±0.1 μs as shown in Fig. 1 (b). The nail plates were exposed to pulses of Yb,Er:Glass laser radiation (λ = 1.54 μm) with energy levels (E) of 30±1, 60±1, and 100±1 mJ at a pulse repetition rate of 1 Hz. The numbers of Yb,Er:Glass laser pulses (N) incident at one point on the nail plate surface were 1, 10, and 100. The diameter of the laser beam in the focal plane was determined by the method of calibrated pinholes. The energy fraction on the output of the 370±10 μm circular pinhole was 86 ± 2%. Waveforms of the laser pulses were obtained with a germanium photodiode and TDS2022B (Tektronix, USA) oscilloscope. The energy of the laser pulses was measured by an OPHIR Nova II (OPHIR Photonics, Israel) power/energy meter that employs the PE50BF-C (OPHIR Photonics, Israel) sensor.

The scheme of the experimental setup for processing the nail plate with Er:YLF laser radiation is shown in Fig. 2(a). The Er:YLF laser operated in free-running mode. The laser was longitudinally pumped by the radiation of a diode laser with a wavelength of 0.98 μm. The Er:YLF laser pulse duration varied from 215 to 280 μs (on the basis), which depended on the power of the diode pumping radiation as shown in Fig. 2(b). The duration of the diode pumping

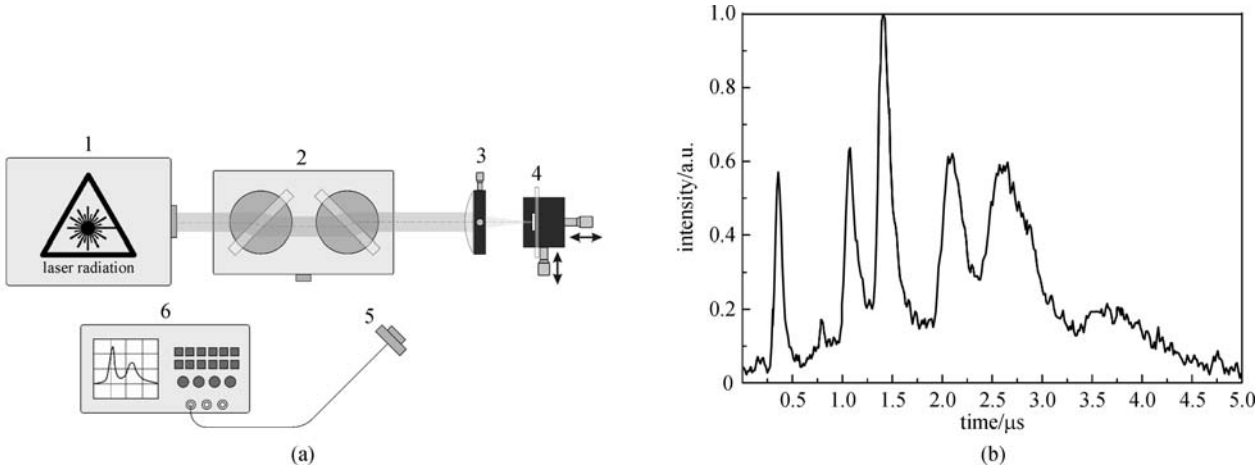

Fig. 1 Experimental setup for processing the nail plate with Yb,Er:Glass laser radiation (a): 1 – Yb,Er:Glass laser, 2 – Fresnel attenuator, 3 – convex lens $F = 11$ mm, 4 – nail plate on the glass substrate, 5 – germanium photodetector, and 6 – oscilloscope; (b) temporal structure of the Yb,Er:Glass laser pulse

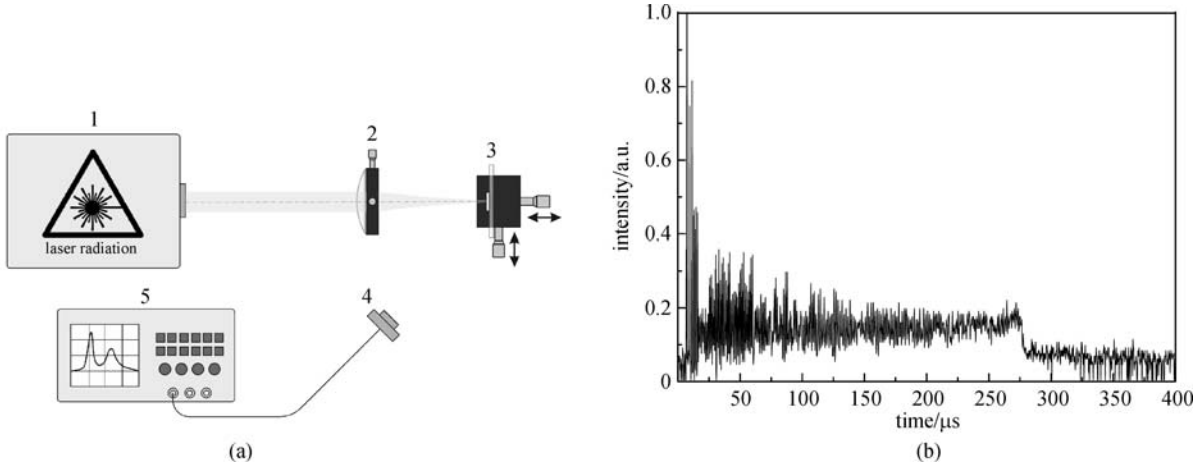

Fig. 2 Experimental setup for processing the nail plate with Er:YLF laser radiation (a): 1 – Er:YLF laser, 2 – convex lens $F = 50$ mm, 3 – nail plate on the glass substrate, 4 – germanium photodetector, and 5 – oscilloscope; (b) temporal structure of the Er:YLF laser pulse ($E = 2$ mJ)

pulse (λ = 0.984 μm) was 300±10 μs and allowed to receive a laser pulse energy of 4±0.01 mJ at a wavelength of 2.81 μm at the maximum pump pulse energy.

The energy levels of the Er:YLF laser pulses (E) were 0.35±0.03, 0.45±0.02, 0.6±0.03, 1±0.01, 2±0.01, 3±0.01, and 4±0.01 mJ at a repetition rate of 30 Hz. The numbers of pulse (N) incident at one point on the nail plate surface were 4, 10, 30, 60, 90, and 120. The beam diameter in the focal plane was determined from the burn obtained on a black photographic paper and was equal to 220±15 μm.

The optical-microscopic registration of the appearance of the laser-induced microdamages of the nail plate was performed under an Axio Scope A1 (Carl Zeiss, Germany) microscope to study the effects of exposing the nail plate to laser radiation at different parameter combinations. The longitudinal sections of the microdamages were then created, and an optical-microscopic recording of their appearance was performed. The longitudinal sections of the nail plate were obtained by gradual abrasive grinding with an abrasive wheel (F320 grit FEPA standard) and low-speed electric motor (2000 r/min). The grinding process was visually monitored under an MSP-1 optical microscope (LOMO, Russia). The obtained images were analyzed to determine the shape and depth of the microcraters and microperforations.

The ablation rate was determined according to Eq. (1):

$$AR = \frac{h}{N}, \tag{1}$$

where h is the microcrater depth and N is the number of pulses incident at one point on the nail plate surface.

The ablation efficiency was determined according to Eq. (2):

$$AE = \frac{h}{N \cdot E}, \quad (2)$$

where h is the microcrater depth, N is the number of pulses incident at one point on the nail plate surface, and E is the laser pulse energy.

For each combination of laser exposure parameters (E and N), 10 implementations were performed on a single sample and standard deviations were determined. Statistical processing of the data was performed using StatGraphics Plus 2.1 (USA).

The nail plate samples were stored at room temperature and 30% relative humidity while studying the effects of the time and storage conditions of the freshly extracted nail plate in open air on the ablation rate by Er:YLF laser radiation (λ = 2.81 μm). Laser exposure was performed 0.5, 1, 2, 4, 8, 48, 72, and 96 h after the extraction of the nail plate on one sample for each combination of E and N to exclude the effect of the chemical differences of nails. After 96 h of storage in open air, the nail plate was placed in distilled water for 1 h at room temperature. After 1 h, the sample was placed in open air, the remaining water was removed from the nail plate surface using a filter paper, and then the sample was exposed to laser radiation again. The Er:YLF pulse energy was 2±0.01 mJ, and the pulse repetition rate was 30 Hz in this case. The numbers of pulses incident at one point on the nail plate surface were 10, 30, 60, 90, and 120. The beam diameter on the nail plate surface was 270±20 μm. The microcrater depth was measured by analyzing the images of the longitudinal sections of microcraters.

3 Results and discussion

The impact of the Yb,Er:Glass and Er:YLF laser pulses on the human nail plate caused bleaching, carbonization, ablation with microcrater formation, and microperforation (Figs. 3 and 4).

The bleaching effect was observed after exposing the nail plate to a single pulse of Yb,Er:Glass laser radiation (λ = 1.54 μm) with energy levels of 60±1 and 100±1 mJ. The appearance of carbonization was recorded after the impact of 10 and 100 Yb,Er:Glass laser pulses with an energy level of 60±1 mJ as well as 10 pulses with an energy level of 100±1 mJ. The effect of removal with microperforation (i.e., the formation of a through microhole in the nail plate) was observed after exposure to 50 pulses with an energy level of 100±1 mJ. Thus, the threshold level of energy density, which is sufficient for the appearance of the bleaching effect under the action of Yb,Er:Glass laser radiation, is 54±3 J/cm^2 (at N = 1), that for the appearance of carbonization is 54±3 J/cm^2 (at N = 10), and that for the microperforation of the nail plate is 91±5 J/cm^2 (at N = 50). The surface of the microcrater walls was rough and had many microcracks. The microcracks can be formed by acoustic waves that arise during the optical breakdown of the nail plate.

The bleaching effect was observed after exposing the nail plate to N = 4 pulses of Er:YLF laser radiation with energy levels of 0.35±0.03 and 0.45±0.02 mJ. Carbonization was observed after the impact of laser pulses with an energy level of 0.6±0.03 mJ at N = 4. This effect can also be observed after exposing the nail plate to 10, 30, 60, 90, and 120 laser pulses with an energy level of 1±0.01 mJ; 10, 30, 60, and 90 pulses with an energy level of 2±0.01 mJ; 10 and 30 pulses with an energy level of 3±0.01 mJ; and 10 pulses with an energy level of 4±0.01 mJ. A conical shape microcrater with a diameter of up to 200 μm was detected when 10 laser pulses with an energy level of 0.6±0.03 mJ affected the nail plate. With the increase in laser pulse energy and pulse number, the microcrater volume increased until the appearance of a through hole. The surface of the microcrater walls was rough and

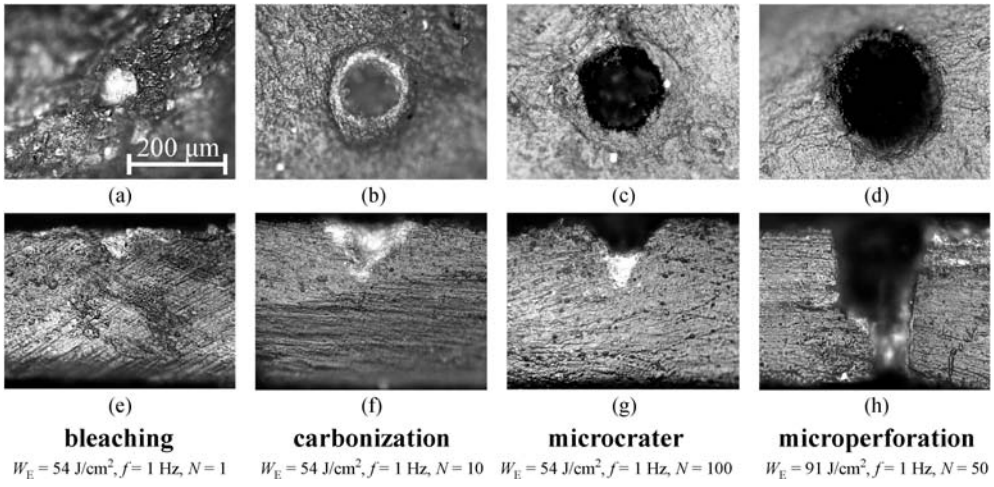

Fig. 3 Images of the nail plates after the impact of Yb,Er:Glass laser: (a)–(d) top view of the microdamages in the nail plates and (e)–(h) longitudinal sections

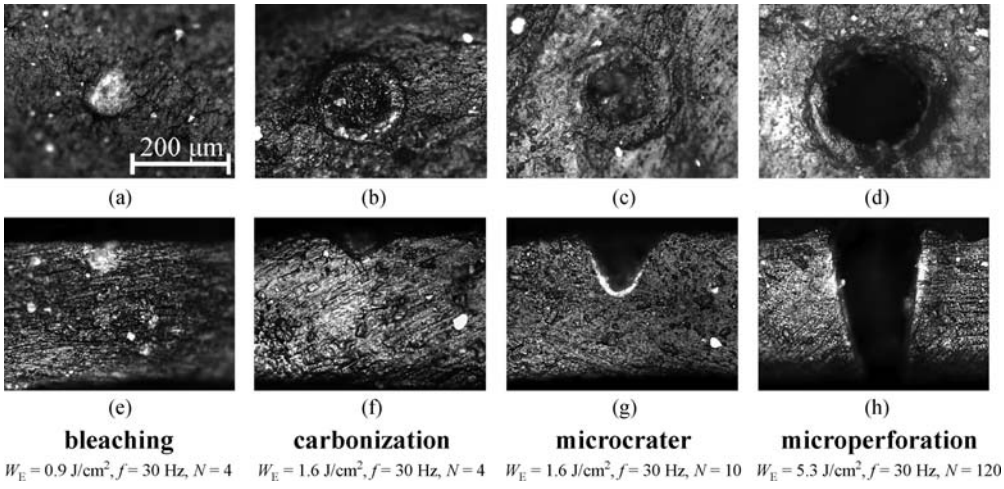

Fig. 4 Images of the nail plates after the impact of Er:YLF laser: (a)–(d) top view of the microdamages in the nail plates and (e)–(h) longitudinal sections

exhibited melting signs. Notably, no microcracks were observed. The effect of ablation with microperforation was observed after exposure to 120 Er:YLF laser pulses with an energy level of 2±0.01 mJ; 60, 90, and 120 pulses with an energy level of 3±0.01 mJ; and 30, 60, 90, and 120 pulses with an energy level of 4±0.01 mJ. Thus, the threshold level of the energy density, which is sufficient for the appearance of the bleaching effect under the action of Er:YLF laser radiation, is approximately 0.9±0.01 J/cm^2 (at N = 4), that for the appearance of carbonization is 1.6±0.2 J/cm^2 (at N = 4), and that for microperforation of the nail plate is 5.3±0.3 J/cm^2 (at N = 120).

The bleaching effect is associated with water evaporation from the surface layers of the nail plate, which leads to the change in optical properties and, as a result, in opacity. Carbonization at the microcrater bottom and walls is probably caused by the destruction of carbon bonds in the keratin, which mostly comprises the nail plate [1].

The rate and efficiency of human nail plate ablation by Yb,Er:Glass laser radiation are shown in Fig. 5.

The maximum ablation rate and ablation efficiency were attained at N = 100 and f = 1 Hz. The maximum ablation rate was 8 μm/pulse (at W_E = 91±2 J/cm^2), and the maximum ablation efficiency was 0.08 μm/mJ (at W_E = 91±2 J/cm^2).

The dependence of the rate of human nail plate ablation by Er:YLF laser radiation on the pulse number (N) is shown in Fig. 6.

The highest rate of the nail plate ablation was observed at N = 4 at E = 4 mJ as shown in Fig. 6. The ablation rate for N = 10 is larger than that for N = 4 at lower energy densities. However, the difference in the ablation rates for

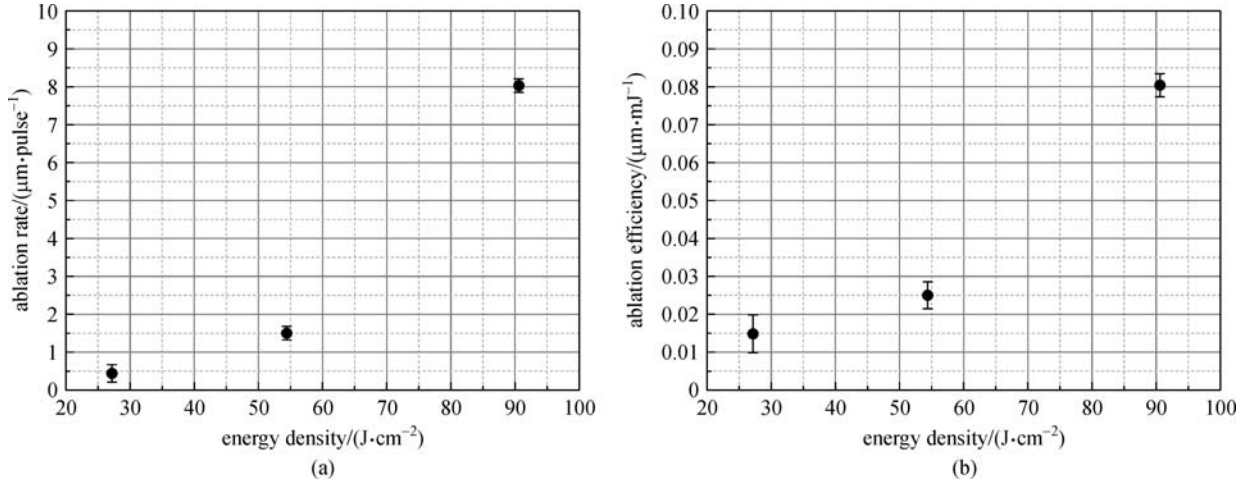

Fig. 5 Dependence of the (a) rate and (b) efficiency of human nail plate ablation on the energy density of Yb,Er:Glass laser radiation (λ = 1.54 μm, N = 100)

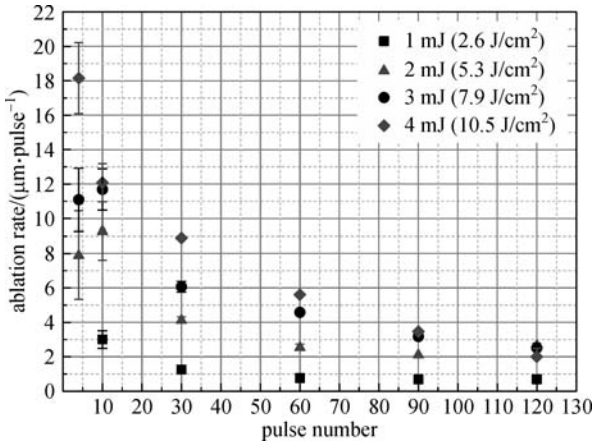

Fig. 6 Dependence of the rate of human nail plate ablation by Er:YLF laser radiation on the pulse number (N)

$N = 4$ and $N = 10$ is excessively small for this case. The data point for $N = 4$ and $E = 1$ mJ is absent in Fig. 6 because we observed only surface damage in this case, and the correct measurement of the ablation crater depth was impossible.

The further increase in the pulse number ($N > 10$) leads to the decrease in ablation rate. We assume that at least two reasons account for such decrease in ablation rate. On the one hand, this scenario may be due to the stepwise displacement of the crater bottom relative to the waist plane of the laser beam at each subsequent pulse. On the other hand, it can be connected with the gradual accumulation of laser destruction products inside the crater, which begin to absorb and scatter the radiation of the following pulses, thereby reducing destruction productivity.

The rate and efficiency of human nail plate ablation by Er:YLF laser radiation are shown in Fig. 7.

The nonlinear dependence of the rate of nail plate ablation on the Er:YLF laser radiation energy density was observed: with the increase in the energy density from 2.6 to 5.3 J/cm^2, a considerable increase in the ablation rate occurred, which slightly changed the speed ablation rate. The maximum ablation rate at $N = 10$ was 12 μm/pulse (at $W_E = 10.5 \pm 0.5$ J/cm^2), and the maximum ablation efficiency was 4.6 μm/mJ (at $W_E = 5.3 \pm 0.3$ J/cm^2).

The microcrater images in the nail plate formed by Er:YLF laser radiation after the sample storage in open air (a–h) and after 1 h of storage in water after 96 h of storage in open air (i) are presented in Fig. 8.

Figure 9 shows the dependence of the microcrater depth (a) and ablation rate (b) of the nail plate by Er:YLF laser radiation on its storage time in open air and after 1 h of storage in water after 96 h of storage in open air.

The depth of microcrater, which can be formed by the Er:YLF laser radiation impact, decreased with the increase in the storage time of the sample in open air as shown in Fig. 9. The maximum change in the microcrater depth occurred within the first 8 h after extraction. The microcrater depth and ablation rate reached their minimum values after 96 h of storage in open air and subsequently did not change. For $N = 90$, the microcrater depth decreased by a maximum of 90±1 μm (i.e., 50% of the initial maximum value). The ablation rate also decreased from 2.1 to 1.1 μm/pulse. After the storing the nail plate in distilled water for an hour, microcraters at approximately the same depth as that of the freshly extracted nail plate were formed.

Such behavior of microcrater depth can be associated with the dehydration–rehydration of the nail plate. Schulz et al. [19] investigated the dependence of the water content in the nail plate on its storage time in open air. Their results showed that the total time of nail rehydration was approximately 20 min, and the complete dehydration of

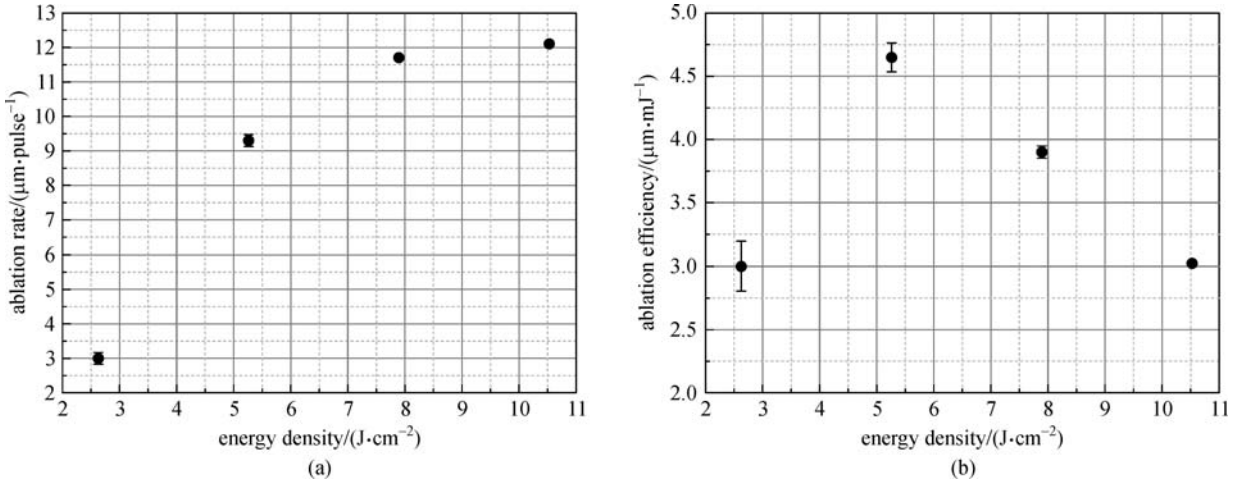

Fig. 7 Dependence of the (a) rate and (b) efficiency of human nail plate ablation on the energy density of Er:YLF laser radiation (λ = 2.81 μm, $N = 10$)

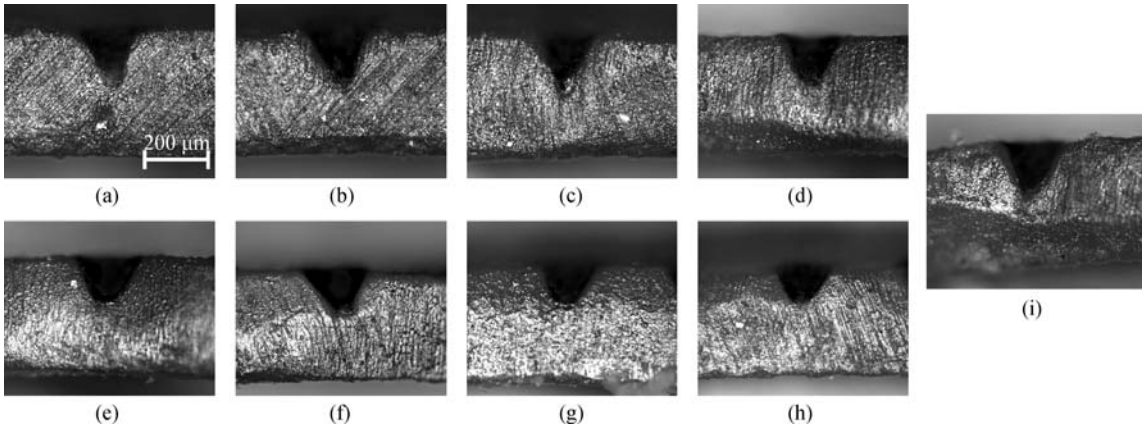

Fig. 8 Microcrater images in the nail plate formed by Er:YLF laser radiation after the sample storage in open air (a – 0.5 h; b – 1 h; c – 2 h; d – 4 h; e – 8 h; f – 48 h; g – 72 h; h – 96 h) and (i) after 1 h of storage in water after 96 h of storage in open air

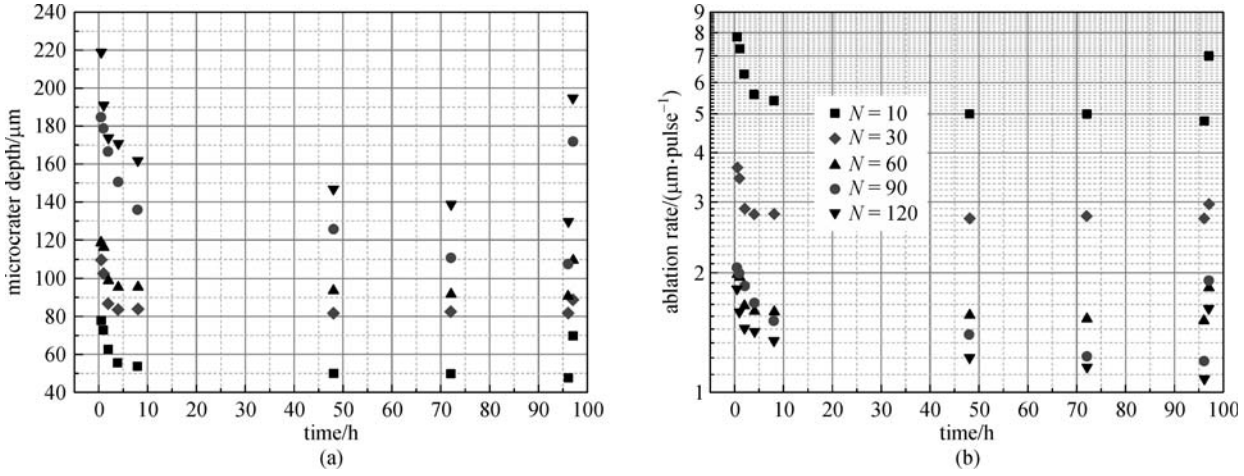

Fig. 9 Dependence of the (a) microcrater depth and (b) ablation rate of the nail plate by Er:YLF laser radiation on its storage time in open air and after 1 h of storage in water after 96 h of storage in open air

the nail plate occurred after 46 h of drying at room temperature and 40% relative humidity. The data on the dynamics of microcrater depth obtained in the present study has a similar form to the dynamics of water content changes in the nail plate during hydration and dehydration presented in Ref. [19]. The Er:YLF laser wavelength belongs to the intense absorption band of water ($\mu_a \approx 7200$ cm^{-1}) [20]; thus, the percentage of water content plays an important role in the nail plate ablation.

4 Conclusion

This study investigated the impact of Yb,Er:Glass (λ = 1.54 μm) and Er:YLF (λ = 2.81 μm) laser radiation on the human nail plate *in vitro*. The laser impact on the nail plate caused bleaching, carbonization, ablation with microcrater formation, and microperforation. The threshold conditions (i.e., laser energy density and pulse number) required for the appearance of each effect were determined. The rate and efficiency of the nail plate ablation by Yb,Er:Glass and Er:YLF laser radiation were experimentally obtained. The effect of dehydration–rehydration on the rate and efficiency of ablation of the nail plate by Er:YLF laser radiation was also studied. The effects of bleaching and carbonization can be in-demand in cosmetology to control the color of the nail plate and create textures. The radiation of both lasers can be used for the microperforation of the nail plate to increase the efficiency of drug delivery in the treatment of onychomycosis and nail psoriasis, as well as to ensure the blood outflow from under the nail plate in the case of subungual hematoma formation.

Our future research will focus on drug penetration through a microhole array in the nail plate. This process can estimate the effect of laser-produced microholes on drug delivery efficiency. After determining the optimal parameters (i.e., size and depth) of microholes and laser radiation required for the formation of such microholes, we

will begin a clinical study of onychomycosis or psoriasis treatment.

Acknowledgements The authors are grateful to the ITMO University (Saint Petersburg, Russia) and Nela Ltd. (Saint Petersburg, Russia) for providing equipment and support to this study. The authors are also grateful to Alexei V. Skrypnik (ITMO University, Saint Petersburg, Russia) for his assistance in the study design.

References

1. Murdan S. Drug delivery to the nail following topical application. International Journal of Pharmaceutics, 2002, 236(1–2): 1–26
2. Saner M V, Kulkarni A D, Pardeshi C V. Insights into drug delivery across the nail plate barrier. Journal of Drug Targeting, 2014, 22(9): 769–789
3. Walters K A, Abdalghafor H M, Lane M E. The human nail–barrier characterisation and permeation enhancement. International Journal of Pharmaceutics, 2012, 435(1): 10–21
4. Elkeeb R, AliKhan A, Elkeeb L, Hui X, Maibach H I. Transungual drug delivery: current status. International Journal of Pharmaceutics, 2010, 384(1–2): 1–8
5. Gain J M, Bogdan V G, Popkov O V, Alekseev S A. Surgery of Ingrown Nail: Monograph. Minsk: Publisher Zmitser Kolas, 2007, 224 (in Russian)
6. Murdan S. Enhancing the nail permeability of topically applied drugs. Expert Opinion on Drug Delivery, 2008, 5(11): 1267–1282
7. Brown M B, Khengar R H, Turner R B, Forbes B, Traynor M J, Evans C R G, Jones S A. Overcoming the nail barrier: a systematic investigation of ungual chemical penetration enhancement. International Journal of Pharmaceutics, 2009, 370(1–2): 61–67
8. Tsai M T, Tsai T Y, Shen S C, Ng C Y, Lee Y J, Lee J D, Yang C H. Evaluation of laser-assisted trans-nail drug delivery with optical coherence tomography. Sensors (Basel), 2016, 16(12): 2111
9. Chiu W S, Belsey N A, Garrett N L, Moger J, Price G J, Delgado-Charro M B, Guy R H. Drug delivery into microneedle-porated nails from nanoparticle reservoirs. Journal of Controlled Release, 2010, 220(Pt A): 98–106
10. Salter S A, Ciocon D H, Gowrishankar T R, Kimball A B. Controlled nail trephination for subungual hematoma. The American Journal of Emergency Medicine, 2006, 24(7): 875–877
11. Adams R M. Effects of mechanical trauma on nails. American Journal of Industrial Medicine, 1985, 8(4–5): 273–280
12. Patel L. Management of simple nail bed lacerations and subungual hematomas in the emergency department. Pediatric Emergency Care, 2014, 30(10): 742–745, quiz 746–748
13. Jelínková H. Lasers for Medical Applications: Diagnostics, Therapy and Surgery. Amsterdam: Elsevier, 2013
14. Neev J, Stuart Nelson J, Critelli M, McCullough J L, Cheung E, Carrasco W A, Rubenchik A M, Da Silva L B, Perry M D, Stuart B C. Ablation of human nail by pulsed lasers. Lasers in Surgery and Medicine, 1997, 21(2): 186–192
15. Morais O O, Costa I M, Gomes C M, Shinzato D H, Ayres G M, Cardoso R M. The use of the Er:YAG 2940 nm laser associated with amorolfine lacquer in the treatment of onychomycosis. Anais Brasileiros de Dermatologia, 2013, 88(5): 847–849
16. Lim E H, Kim H R, Park Y O, Lee Y, Seo Y J, Kim C D, Lee J H, Im M. Toenail onychomycosis treated with a fractional carbon-dioxide laser and topical antifungal cream. Journal of the American Academy of Dermatology, 2014, 70(5): 918–923
17. Myers M J, Myers J A, Roth F, Guo B, Hardy C R, Myers S, Carrabba A, Trywick C B S, Griswold J R, Mazzochi A. Treatment of toe nail fungus infection using an AO Q-switched eye-safe erbium glass laser at 1534 nm. Proceedings of SPIE, 2013, 8565: 85650W1–9
18. Kozarev J. Novel laser therapy in treatment of onychomycosis. Journal of the Laser and Health Academy, 2010, 2010(1): 1–8
19. Schulz B, Chan D, Bäckström J, Rübhausen M, Wittern K P, Wessel S, Wepf R, Williams S. Hydration dynamics of human fingernails: an ellipsometric study. Physical Review E, Statistical, Nonlinear, and Soft Matter Physics, 2002, 65(6): 061913
20. Jacques S L. Optical properties of biological tissues: a review. Physics in Medicine and Biology, 2013, 58(11): R37–R61

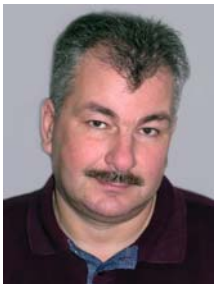

Andrey V. Belikov graduated in 1990 from Saint-Petersburg Institute of Fine Mechanics and Optics (SPIFMO), specialty optics. His professional experience and positions: 1990–1993, post-graduate student of Quantum Electronics and Biomedical Optics Department of SPIFMO; 1993–2002, Ph.D., senior researcher of Quantum Electronics and Biomedical Optics Department of SPIFMO; 2002–2013, associate Professor of Laser Technique and Biomedical Optics Department of Saint-Petersburg State University of Information Technologies, Mechanics and Optics (SPb SU ITMO); 2013–2015, Professor of Laser Technique and Biomedical Optics Department of Saint-Petersburg National Research University of Information Technologies, Mechanics and Optics (ITMO University); 2015–2016, Professor of Laser Technologies and Laser Technique Department of ITMO University; 2016–present, Professor of Laser Technologies and Systems Department of ITMO University.

His professional activities: 6 international projects (optics for medicine), more than 20 international congresses, 6 invited lectures. His research interests are biomedical optics, physics of interaction of light with materials. He has published more than 180 papers.

Andrey N. Sergeev received his Bachelor degree in photonics and optical information technologies from St. Petersburg State University of Information Technologies, Mechanics and Optics in 2009; Master degree in photonics and optical information technologies from St. Petersburg National Research University of Information Technologies, Mechanics and Optics (ITMO University) in 2011; Ph.D. degree in quantum electronics from ITMO University in 2014. His Ph.D. thesis theme was “Design of minilasers for study of information recording in photosensitive materials by methods of nonlinear optics”. Since 2014, he is Assistant Professor at Laser Technologies and Systems Department

of ITMO University. His research interests are DPSS lasers, minilasers, microchip lasers, lasers for biomedical applications, nonlinear optics, optical information recording, optical information technologies. His professional activities: participation in 6 international conferences. He has published over 20 papers.

Sergey N. Smirnov received his Bachelor degree in technical physics from St. Petersburg National Research University of Information Technologies, Mechanics and Optics (ITMO University) in 2013; Master degree in laser instrumentation and technologies from ITMO University in 2015. His Master's thesis was "High-power pulsed diode-pumped laser of eye-safe spectral range". Since 2015, he is Ph.D. student of Laser Technologies and Systems department of ITMO University (specialty – quantum electronics). His professional activities: participation in 7 conferences, including 2 all-Russian and 2 international. His research interests are solid-state lasers, laser and optical systems for biomedical applications, laser-matter interaction, optoacoustics, tissue optics. He has published 5 papers.

Anastasia D. Tavalinskaya completed upper secondary education, currently – fourth year student of St. Petersburg University of Information Technologies, Mechanics and Optics (ITMO University). Since 2013, she is a student of Laser Technologies and Systems Department of ITMO University. Her professional activities: participation in 2 all-Russian conferences. Her research interests are laser technology and biomedical optics.